BULETINUL ACADEMIEI DE ŞTIINŢE
A REPUBLICII MOLDOVA. MATEMATICA
Number 1(59), 2009, Pages 3–21
ISSN 1024–7696

Optimal control for one complex dynamic system, I

Alla Albu, Vladimir Zubov

Abstract. The optimal control problem of the metal solidification in casting is considered. The process is modeled by a three-dimensional two-phase initial-boundary value problem of the Stefan type. A numerical algorithm is presented for solving the direct problem. The optimal control problem was solved numerically using the gradient method. The gradient of the cost function was found with the help of conjugate problem. The discreet conjugate problem was posed with the help of Fast Automatic Differentiation technique.

Mathematics subject classification: 49J20, 93C20.
Keywords and phrases: Heat conduction, Stefan problem, finite-difference scheme, optimal control, gradient method, Fast Automatic Differentiation technique.

1 Introduction

An important class of heat transfer problems is that describing processes in which the substance under study undergoes phase transitions accompanied by heat release or absorption (Stefan problems). A key feature of these problems is that they involve a moving interface between two phases (liquid and solid). The law of motion of the interface is unknown in advance and is to be determined. It is on this interface that heat release or absorption associated with phase transitions occurs. The thermal properties of the substance on the different sides of the moving interface can be different. Problems of this class are noticeably more complicated than those not involving phase transitions.

We consider an interesting problem of this class, namely, the optimal control of the process of solidification in metal casting. Figure 1 shows the experimental setup for metal solidification. It consists of upper and lower parts. The upper part consists of a furnace with a mold moving inside. The lower part is a cooling bath consisting of a large tank filled with liquid aluminum whose temperature is somewhat higher than the aluminum melting point. The cooling of liquid metal in the furnace proceeds as follows. On the one hand, the mold is slowly immersed in the low-temperature liquid aluminum, which causes the solidification of the metal. On the other hand, the mold gains heat from the walls of the furnace, which prevents the solidification process from proceeding too fast. The optimal control problem is to choose a regime of metal cooling and solidification at which the solidification front has a preset shape (or is close to it) and moves sufficiently slowly (at a speed close to the preset one).

An important part of the optimal control problem is the direct problem (of finding the temperature at each point of the metal and determining the solidification

front). We describe the mathematical formulation of the direct problem, its finite-difference approximation, and a numerical algorithm for solving the direct problem. The problem was studied for an object of the simplest shape (a parallelepiped) and for an actual object of practice interest (Fig. 2). While discussing the numerical results, we give primary attention to the evolution of the solidification front and to how it is affected by the parameters of the problem.

The control function was approximated by a piecewise constant function. The minimum value of a cost function was finding numerically with use of gradient methods. The gradient of the cost function was found with the help of conjugate problem. The discreet conjugate problem was posed with the help of Fast Automatic Differentiation technique.

2 Mathematical formulation of the problem

The following optimal control problem of metal solidification in casting is considered.

A mold with specified outer and inner boundaries is filled with liquid metal (the longitudinal projections of an actual mold are presented in Fig. 2). The hatched area in the Fig. 2 depicts the mold wall, and the internal unhatched area shows the inside space filled with metal. The mold and the metal inside it are heated up to prescribed temperatures T_{form} and T_{met}, respectively. Next, the mold filled with metal (which is hereafter referred to as the object) begins to cool gradually under varying surrounding conditions. The different parts of the mold's outer boundary are under different thermal conditions (the laws of heat transfer with the surroundings are different in these parts). Moreover, the thermal conditions affecting the parts vary with time.

The process of cooling the object is described by the equation:

$$\rho C\frac{\partial T}{\partial t} = \frac{\partial}{\partial x}\left(K\frac{\partial T}{\partial x}\right) + \frac{\partial}{\partial y}\left(K\frac{\partial T}{\partial y}\right) + \frac{\partial}{\partial z}\left(K\frac{\partial T}{\partial z}\right), \qquad (x,y,z) \in Q. \quad (1)$$

Here x, y, and z are the Cartesian coordinates of a point; t is time; Q is a domain with a piecewise smooth boundary Γ; $T(x,y,z,t)$ is the substance temperature at the point with coordinates (x,y,z) at time t; ρ, C and K are the density, heat capacity, and thermal conductivity of the substance respectively.

The conditions of heat transfer with the surrounding medium are set on the boundary Γ of Q. As was mentioned above, these conditions depend on the given surface point and time. However, all the heat transfer conditions can be written in the general form:

$$\tilde{\alpha}T + \tilde{\beta}T_{\mathbf{n}} = \tilde{\gamma}. \quad (2)$$

Here $\tilde{\alpha}$, $\tilde{\beta}$, and $\tilde{\gamma}$ are given functions of the coordinates (x,y,z) of a point on Γ and the temperature $T(x,y,z,t)$, and $\dfrac{\partial T}{\partial \mathbf{n}} = T_{\mathbf{n}}$ is the derivative of T in the direction $\mathbf{n}$ – the external normal to the surface Γ. It should be noted that the coefficients

ρ, C and K in (1) and (2) are different for the metal and the mold. They have the form:

$$K(T) = \begin{cases} K_1(T), & (x,y,z) \in \text{metal}, \\ K_2(T), & (x,y,z) \in \text{mold}, \end{cases}$$

$$K_1(T) = \begin{cases} k_S, & T < T_1, \\ \dfrac{k_L - k_S}{T_2 - T_1} T + \dfrac{k_S T_2 - k_L T_1}{T_2 - T_1}, & T_1 \le T < T_2, \\ k_L, & T \ge T_2, \end{cases}$$

$$K_2(T) = \begin{cases} k_{\Phi_1}, & T \le T_3, \\ k_{\Phi_2}, & T > T_3, \end{cases}$$

$$\rho(T) = \begin{cases} \rho_1(T), & (x,y,z) \in \text{metal}, \\ \rho_\Phi, & (x,y,z) \in \text{mold}, \end{cases} \qquad \rho_1(T) = \begin{cases} \rho_S, & T < T_1, \\ \rho_L, & T \ge T_2, \end{cases}$$

$$C(T) = \begin{cases} C_1(T), & (x,y,z) \in \text{metal}, \\ c_\Phi, & (x,y,z) \in \text{mold}, \end{cases} \qquad C_1(T) = \begin{cases} c_S, & T < T_1, \\ c_L, & T \ge T_2. \end{cases}$$

The constants c_S, c_L, c_Φ, ρ_S, ρ_L, ρ_Φ, k_S, k_L, k_{Φ_1}, k_{Φ_2}, T_1, T_2, and T_3 in these formulas are assumed to be known.

It should be noted that the thermodynamic coefficients have a jump at the metal-mold interface. Two conditions are set at this surface, namely, the temperature and the heat flux must be continuous.

Note also that the metal can be simultaneously in two phases: solid and liquid. The domain separating the phases is determined by a narrow range of temperatures $[T_1, T_2]$, in which ρ, C and K change very rapidly.

Thus, the solution to the direct problem consists in determining a function $T(x,y,z,t)$ that satisfies Eq. (1) in Q, conditions (2) on the outer boundary Γ of Q, and the continuity conditions for the temperature and the heat flux at the metal-mold interface.

The optimal control problem is to choose a regime of metal cooling and solidification at which the solidification front has a preset shape or is close to it (namely, a plane orthogonal to the vertical axis of the object) and moves sufficiently slowly (at a speed close to the preset one). The evolution of the solidification front is affected by numerous parameters (for example, by the furnace temperature, the liquid aluminum temperature, the depth to which the object is immersed in the liquid aluminum, the speed at which the mold moves relative to the furnace, etc.). The solidification front as a function of the velocity of the object is of special interest in practice.

The speed $\widetilde{u}(t)$ of the displacement of foundry mold in the melting furnace was chosen as the control $U(t)$. The cost function is next:

$$I(U) = \frac{1}{t_2 - t_1} \int\limits_{t_1}^{t_2} \iint\limits_{S} [Z_{pl}(x,y,t) - z_*(t)]^2 dx dy dt. \tag{3}$$

Here t_1 is the time, when the crystallization front is conceived; t_2 is the time, when the crystallization of metal completes; $(x, y, Z_{pl}(x, y, t))$ are the real coordinates of the interface at the time t; $(x, y, Z_*(t))$ are the desired coordinates of the interface at the time t; S is the cross section of the mold which is filled by metal. The control function may be restricted by some prescribed functions $U_1(t)$ and $U_2(t)$: $U_1(t) \le U(t) \le U_2(t)$.

3 Numerical algorithm for solving the direct problem

The time's grid is introduced by relations: $\{t^j\}, \quad j = \overline{0, J}$, with the mesh sizes $\tau^j = t^j - t^{j-1}, \quad j = \overline{1, J}$.

The object being investigated is approximated by the body, which consists of a finite number of rectangular parallelepipeds. The approximating body is placed wholly into a certain large parallelepiped. For convenience in the further consideration let us introduce the coordinate system, connected with the moving foundry mold (see, Fig. 1). Axis Oz let direct vertically upward, the axis Ox will arrange in the horizontal plane and will direct from left to right, and the axis Oy let select so the coordinate system $Oxyz$ would be right. The beginning O of this coordinate system is compatible with the left, nearest to us vertex of the large parallelepiped, situated on its bottom. In this large parallelepiped a basic non-uniform rectangular grid is introduced:

$$\{x_n\},\ n = \overline{0, N}; \qquad \{y_i\},\ i = \overline{0, I}; \qquad \{z_l\},\ l = \overline{0, L};$$

with the mesh sizes: $h_n^x = x_{n+1} - x_n,\ \ n = \overline{0, N-1}; \quad h_i^y = y_{i+1} - y_i,\ \ i = \overline{0, I-1}; \quad h_l^z = z_{l+1} - z_l,\ \ l = \overline{0, L-1}$. This grid is introduced in such a way that all external surfaces of the approximating body, and also surfaces which separate metal and form would coincide with the grid surfaces.

Besides the basic grid, the auxiliary grid is built whose surfaces are parallel to the surfaces of the basic grid and are displaced relative to it with a half-step in all directions:

$$\widetilde{x}_0 = x_0; \quad \widetilde{x}_n = x_{n-1} + h_{n-1}^x/2; \quad n = \overline{1, N}; \quad \widetilde{x}_{N+1} = x_N;$$

$$\widetilde{y}_0 = y_0; \quad \widetilde{y}_i = y_{i-1} + h_{i-1}^y/2; \quad i = \overline{1, I}; \quad \widetilde{y}_{I+1} = y_I;$$

$$\widetilde{z}_0 = z_0; \quad \widetilde{z}_l = z_{l-1} + h_{l-1}^z/2; \quad l = \overline{1, L}; \quad \widetilde{z}_{L+1} = z_L.$$

The planes $x = \widetilde{x}_n, y = \widetilde{y}_i$, and $z = \widetilde{z}_l$ split the object into elementary volumes, or elementary cells. An elementary cell is assigned by the indices (n, i, l) if the cell's vertex nearest to the coordinates origin O coincides with the nodal point $(\widetilde{x}_n, \widetilde{y}_i, \widetilde{z}_l)$. The volume of such an elementary cell is denoted by V_{nil} and its outer surface is denoted by S_{nil}.

Let us assume that the temperature of the medium within an elementary cell is independent of the spatial coordinates but depends on time. Denote this temperature by $T_{nil}(t)$.

Any elementary cell is either completely filled with a single medium (metal or mold) or some part is filled with one medium and the remaining part with the other. Let V^1_{nil} denote the part of V_{nil} filled with the metal and V^2_{nil} denote the part of V_{nil} filled with the mold material. Similarly, S^1_{nil} is the part of S_{nil} that is adjacent to V^1_{nil} and S^2_{nil} is the part of S_{nil} that is adjacent to V^2_{nil}.

The algorithm that solves the direct problem is based on the heat balance law and on the reformulation from the problem in terms of temperature to terms of enthalpy.

For any volume V with outer boundary S, we have the heat balance law

$$\iiint\limits_V \left[H\left(T(x,y,z,t^{j+1})\right) - H\left(T(x,y,z,t^j)\right)\right] dV = \int\limits_{t^j}^{t^{j+1}} \iint\limits_S K(T) T_{\mathbf{n}} ds dt. \tag{4}$$

Here, $H\left(T(x,y,z,t)\right)$ is the enthalpy function defined as:

$$H\left(T(x,y,z,t)\right) = \begin{cases} H_1(T), & (x,y,z) \in \text{metal}, \\ H_2(T), & (x,y,z) \in \text{mold}, \end{cases}$$

$$H_1(T) = \begin{cases} \rho_S c_S T, & T < T_1, \\ \dfrac{\rho_S c_S (T_2 - T_1) + \rho_S \gamma}{T_2 - T_1} T - \dfrac{\rho_S \gamma T_1}{T_2 - T_1}, & T_1 \le T < T_2, \\ \rho_L c_L (T - T_2) + \rho_S c_S T_2 + \rho_S \gamma, & T \ge T_2, \end{cases} \tag{5}$$

$$H_2(T) = \rho_\Phi c_\Phi T. \tag{6}$$

Then relation (4) written for an elementary cell indexed by (n,i,l) becomes:

$$\left[V^1_{nil} H_1\left(T^{j+1}_{nil}\right) + V^2_{nil} H_2\left(T^{j+1}_{nil}\right)\right] - \left[V^1_{nil} H_1\left(T^{j}_{nil}\right) + V^2_{nil} H_2\left(T^{j}_{nil}\right)\right] =$$

$$= \int\limits_{t^j}^{t^{j+1}} \left[\iint\limits_{S^1_{nil}} K_1(\widetilde{T}_{nil}(t))(\widetilde{T}_{\mathbf{n}}(t))_{nil} ds + \iint\limits_{S^2_{nil}} K_2(\widetilde{T}_{nil}(t))(\widetilde{T}_{\mathbf{n}}(t))_{nil} ds \right] dt. \tag{7}$$

Here $T^j_{nil} = T_{nil}(t^j)$, $K_1(\widetilde{T}_{nil}(t))(\widetilde{T}_{\mathbf{n}}(t))_{nil}$, and $K_2(\widetilde{T}_{nil}(t))(\widetilde{T}_{\mathbf{n}}(t))_{nil}$ are the heat flux densities through the cell surface.

The subsequent transformations of (7) are similar to those proposed in [1–3] and further developed in [4–7].

Let $M_{nil} = V^1_{nil}/V_{nil}$ be the metal volume fraction in the elementary cell indexed by (n,i,l) and $\Phi_{nil} = V^2_{nil}/V_{nil}$ be the mold volume fraction in this elementary cell.

Define the aggregate enthalpy density in the cell indexed by (n,i,l) at the time t^j as $E^j_{nil} = M_{nil} H_1(T^j_{nil}) + \Phi_{nil} H_2(T^j_{nil})$. Taking into account (5) and (6), which define $H_1(T)$ and $H_2(T)$, we obtain an expression for $E(T^j_{nil})$:

$$E^j_{nil} \equiv E(T^j_{nil}) = \begin{cases} a_{nil} T^j_{nil}, & T^j_{nil} < T_1, \\ b^1_{nil} T^j_{nil} - b^2_{nil}, & T_1 \le T^j_{nil} < T_2, \\ d^1_{nil} T^j_{nil} + d^2_{nil}, & T^j_{nil} \ge T_2, \end{cases}$$

where

$$a_{nil} = M_{nil}\rho_S c_S + \Phi_{nil}\rho_\Phi c_\Phi,$$
$$b^1_{nil} = M_{nil}(\rho_S c_S + \rho_S\gamma/(T_2 - T_1)) + \Phi_{nil}\rho_\Phi c_\Phi, \quad b^2_{nil} = M_{nil}\rho_S\gamma T_1/(T_2 - T_1),$$
$$d^1_{nil} = M_{nil}\rho_L c_L + \Phi_{nil}\rho_\Phi c_\Phi, \qquad d^2_{nil} = M_{nil}(\rho_S\gamma + (\rho_S c_S - \rho_L c_L)T_2).$$

Now, the temperature is defined as a function of E^j_{nil} (this function is the inverse of $E(T^j_{nil})$):

$$T^j_{nil} \equiv \beta(E^j_{nil}) = \beta^j_{nil} = \begin{cases} \dfrac{1}{a_{nil}}E^j_{nil}, & E^j_{nil} < a_{nil}T_1, \\ \dfrac{1}{b^1_{nil}}E^j_{nil} + \dfrac{b^2_{nil}}{b^1_{nil}}, & a_{nil}T_1 \le E^j_{nil} < d^1_{nil}T_2 + d^2_{nil}, \\ \dfrac{1}{d^1_{nil}}E^j_{nil} - \dfrac{d^2_{nil}}{d^1_{nil}}, & E^j_{nil} \ge d^1_{nil}T_2 + d^2_{nil}. \end{cases}$$

The functions $K_1(T^j_{nil})$ and $K_2(T^j_{nil})$ can be expressed in terms of enthalpy:

$$K_1(T^j_{nil}) \equiv \Omega_1(E^j_{nil}) = \begin{cases} k_S, & E^j_{nil} < \rho_S c_S T_1 \equiv E_1, \\ \dfrac{k_L - k_S}{E_2 - E_1}E^j_{nil} + \dfrac{k_S E_2 - k_L E_1}{E_2 - E_1}, & E_1 \le E^j_{nil} < \rho_S(c_S T_2 + \gamma) \equiv E_2, \\ k_L, & E^j_{nil} \ge E_2, \end{cases}$$

$$K_2(T^j_{nil}) \equiv \Omega_2(E^j_{nil}) = \begin{cases} k_{\Phi_1}, & E^j_{nil} < \rho_\Phi c_\Phi(T_3 - \delta) \equiv E_3, \\ \dfrac{k_{\Phi_2} - k_{\Phi_1}}{E_4 - E_3}E^j_{nil} + \dfrac{k_{\Phi_1}E_4 - k_{\Phi_2}E_3}{E_4 - E_3}, & E_3 \le E^j_{nil} < \rho_\Phi c_\Phi(T_3 + \delta) \equiv E_4, \\ k_{\Phi_2}, & E^j_{nil} \ge E_4, \end{cases}$$

where $\delta << T_3$.

In (7), we proceed from the variable $T_{nil}(t)$ to $E_{nil}(t)$ and obtain:

$$V_{nil} \cdot (E^{j+1}_{nil} - E^j_{nil}) = \int\limits_{t^j}^{t^{j+1}} \left[\iint\limits_{S^1_{nil}} A_1(\widetilde{E}_{nil}(t))ds + \iint\limits_{S^2_{nil}} A_2(\widetilde{E}_{nil}(t))ds \right] dt, \qquad (8)$$

where $A_1(\widetilde{E}_{nil}(t)) = \Omega_1(\widetilde{E}_{nil}(t))\beta_{\mathbf{n}}(\widetilde{E}_{nil}(t)), \quad A_2(\widetilde{E}_{nil}(t)) = \Omega_2(\widetilde{E}_{nil}(t))\beta_{\mathbf{n}}(\widetilde{E}_{nil}(t))$.

We introduce the notation

$$E^{j+1/3}_{nil} = E_{nil}\left(t^j + \frac{\tau^{j+1}}{3}\right), \quad E^{j+2/3}_{nil} = E_{nil}\left(t^j + \frac{2\tau^{j+1}}{3}\right).$$

The time discretization of Eq.(8) is based on the Peaceman-Rachford scheme (see [8]):

$$V_{nil} \cdot (E^{j+1}_{nil} - E^j_{nil}) = \frac{2\tau^{j+1}}{3}\left[\iint\limits_{S^{1x+}_{nil} \bigcup S^{1x-}_{nil}} A_1(E^{j+\frac{1}{3}}_{nil})ds + \iint\limits_{S^{2x+}_{nil} \bigcup S^{2x-}_{nil}} A_2(E^{j+\frac{1}{3}}_{nil})ds \right] + \frac{\tau^{j+1}}{3} \times$$

$$\times\left[\iint\limits_{S_{nil}^{1x+}\bigcup S_{nil}^{1x-}}A_1(E_{nil}^{j+\frac{2}{3}})ds+\iint\limits_{S_{nil}^{2x+}\bigcup S_{nil}^{2x-}}A_2(E_{nil}^{j+\frac{2}{3}})ds+\iint\limits_{S_{nil}^{1y+}\bigcup S_{nil}^{1y-}}A_1(E_{nil}^{j})ds+\iint\limits_{S_{nil}^{2y+}\bigcup S_{nil}^{2y-}}A_2(E_{nil}^{j})ds\right]+$$

$$+\frac{2\tau^{j+1}}{3}\left[\iint\limits_{S_{nil}^{1y+}\bigcup S_{nil}^{1y-}}A_1(E_{nil}^{j+\frac{2}{3}})ds+\iint\limits_{S_{nil}^{2y+}\bigcup S_{nil}^{2y-}}A_2(E_{nil}^{j+\frac{2}{3}})ds\right]+ \tag{9}$$

$$+\frac{\tau^{j+1}}{3}\left[\iint\limits_{S_{nil}^{1z+}\bigcup S_{nil}^{1z-}}A_1(E_{nil}^{j})ds+\iint\limits_{S_{nil}^{2z+}\bigcup S_{nil}^{2z-}}A_2(E_{nil}^{j})ds+\iint\limits_{S_{nil}^{1z+}\bigcup S_{nil}^{1z-}}A_1(E_{nil}^{j+\frac{1}{3}})ds+\right.$$

$$\left.+\int\limits_{S_{nil}^{2z+}\bigcup S_{nil}^{2z-}}A_2(E_{nil}^{j+\frac{1}{3}})ds+\int\limits_{S_{nil}^{1z+}\bigcup S_{nil}^{1z-}}A_1(E_{nil}^{j+1})ds+\int\limits_{S_{nil}^{2z+}\bigcup S_{nil}^{2z-}}A_2(E_{nil}^{j+1})ds\right].$$

Here S_{nil}^{1x+} denotes the part of S_{nil}^{1} that belongs to the plane $x=\widetilde{x}_{n+1}$ and S_{nil}^{1x-} denotes the part of S_{nil}^{1} that belongs to the plane $x=\widetilde{x}_{n}$. $S_{nil}^{1y+},...,S_{nil}^{1z-}$, $S_{nil}^{2x+},...,S_{nil}^{2z-}$ are defined in a similar fashion.

We simultaneously add and subtract $V_{nil}E_{nil}^{j+1/3}$ and $V_{nil}E_{nil}^{j+2/3}$ on the left-hand side of (9) and split this equation into three (with respect to the directions x, y and z), thus, forming the following three subproblems:

$$\left(j=\overline{0,J-1},\ n=\overline{0,N},\ i=\overline{0,I},\ l=\overline{0,L}\right)$$

$$\mathbf{x-direction}$$

$$V_{nil}\cdot(E_{nil}^{j+\frac{1}{3}}-E_{nil}^{j})=\frac{\tau^{j+1}}{3}\left[\iint\limits_{S_{nil}^{1x+}\bigcup S_{nil}^{1x-}}A_1(E_{nil}^{j+\frac{1}{3}})ds+\iint\limits_{S_{nil}^{2x+}\bigcup S_{nil}^{2x-}}A_2(E_{nil}^{j+\frac{1}{3}})ds+\right.$$

$$\left.+\iint\limits_{S_{nil}^{1y+}\bigcup S_{nil}^{1y-}}A_1(E_{nil}^{j})ds+\iint\limits_{S_{nil}^{2y+}\bigcup S_{nil}^{2y-}}A_2(E_{nil}^{j})ds+\iint\limits_{S_{nil}^{1z+}\bigcup S_{nil}^{1z-}}A_1(E_{nil}^{j})ds+\iint\limits_{S_{nil}^{2z+}\bigcup S_{nil}^{2z-}}A_2(E_{nil}^{j})ds\right];$$

$$\mathbf{y-direction}$$

$$V_{nil}\cdot(E_{nil}^{j+\frac{2}{3}}-E_{nil}^{j+\frac{1}{3}})=\frac{\tau^{j+1}}{3}\left[\iint\limits_{S_{nil}^{1y+}\bigcup S_{nil}^{1y-}}A_1(E_{nil}^{j+\frac{2}{3}})ds+\iint\limits_{S_{nil}^{2y+}\bigcup S_{nil}^{2y-}}A_2(E_{nil}^{j+\frac{2}{3}})ds+\right.$$

$$\left.+\iint\limits_{S_{nil}^{1x+}\bigcup S_{nil}^{1x-}}A_1(E_{nil}^{j+\frac{1}{3}})ds+\iint\limits_{S_{nil}^{2x+}\bigcup S_{nil}^{2x-}}A_2(E_{nil}^{j+\frac{1}{3}})ds+\iint\limits_{S_{nil}^{1z+}\bigcup S_{nil}^{1z-}}A_1(E_{nil}^{j+\frac{1}{3}})ds+\iint\limits_{S_{nil}^{2z+}\bigcup S_{nil}^{2z-}}A_2(E_{nil}^{j+\frac{1}{3}})ds\right];$$

z − direction

$$V_{nil}\cdot(E_{nil}^{j+1}-E_{nil}^{j+\frac{2}{3}})=\frac{\tau^{j+1}}{3}\left[\iint\limits_{S_{nil}^{1z+}\bigcup S_{nil}^{1z-}}A_1(E_{nil}^{j+1})ds+\iint\limits_{S_{nil}^{2z+}\bigcup S_{nil}^{2z-}}A_2(E_{nil}^{j+1})ds+\right.$$

$$\left.+\iint\limits_{S_{nil}^{1x+}\bigcup S_{nil}^{1x-}}A_1(E_{nil}^{j+\frac{2}{3}})ds+\iint\limits_{S_{nil}^{2x+}\bigcup S_{nil}^{2x-}}A_2(E_{nil}^{j+\frac{2}{3}})ds+\iint\limits_{S_{nil}^{1y+}\bigcup S_{nil}^{1y-}}A_1(E_{nil}^{j+\frac{2}{3}})ds+\iint\limits_{S_{nil}^{2y+}\bigcup S_{nil}^{2y-}}A_2(E_{nil}^{j+\frac{2}{3}})ds\right].$$

The thermal conductivities $\Omega_1(\widetilde{E}_{nil}^j)$ and $\Omega_2(\widetilde{E}_{nil}^j)$ on internal surfaces of the elementary cell are approximated as:

$$\Omega_1(\widetilde{E}_{nil}^j)\Big|_{S_{nil}^{1x+}}=\frac{\Omega_1(E_{nil}^j)+\Omega_1(E_{n+1,il}^j)}{2}\equiv R_n^j,$$

$$\Omega_1(\widetilde{E}_{nil}^j)\Big|_{S_{nil}^{1x-}}=\frac{\Omega_1(E_{n-1,il}^j)+\Omega_1(E_{nil}^j)}{2}\equiv R_{n-1}^j,$$

$$\Omega_1(\widetilde{E}_{nil}^j)\Big|_{S_{nil}^{1y+}}=\frac{\Omega_1(E_{nil}^j)+\Omega_1(E_{n,i+1,l}^j)}{2}\equiv \widehat{R}_i^j,$$

$$\Omega_1(\widetilde{E}_{nil}^j)\Big|_{S_{nil}^{1y-}}=\frac{\Omega_1(E_{nil}^j)+\Omega_1(E_{n,i-1,l}^j)}{2}\equiv \widehat{R}_{i-1}^j.$$

The notations $\widetilde{R}_l^j$ and $\widetilde{R}_{l-1}^j$ for the surfaces S_{nil}^{1z+} and S_{nil}^{1z-} and the notations B_n^j, B_{n-1}^j, $\widehat{B}_i^j$, $\widehat{B}_{i-1}^j$, $\widetilde{B}_l^j$, and $\widetilde{B}_{l-1}^j$ for $\Omega_2(\widetilde{E}_{nil}^j)$ are introduced in a similar manner.

For simplicity, the subsequent presentation of the algorithm is given for the simplest domain – a rectangular parallelepiped.

The derivative $\beta_{\mathbf{n}}(E)$ in the outward normal direction $\mathbf{n}$ on Γ are approximated by the formula: $\beta_{\mathbf{n}}(E)=(\nabla\beta,\mathbf{n})$, where, for example,

$$\beta_{\mathbf{n}}(E_{nil}^j)\Big|_{S_{nil}^{1x+}}=\frac{\beta_{n+1,il}^j-\beta_{nil}^j}{h_n^x},\quad \left(n=\overline{0,N-1};i=\overline{0,I};l=\overline{0,L}\right),$$

$$\beta_{\mathbf{n}}(E_{nil}^j)\Big|_{S_{nil}^{1x-}}=-\frac{\beta_{nil}^j-\beta_{n-1,il}^j}{h_{n-1}^x},\quad \left(n=\overline{1,N};i=\overline{0,I};l=\overline{0,L}\right).$$

With the notation introduced, the spatial approximation of the first subproblem inside the domain under consideration can be written as:

$$E_{nil}^{j+\frac{1}{3}}-E_{nil}^j=\omega_{nil}^{j+1}\left[\left(S_{nil}^{1x+}R_n^{j+\frac{1}{3}}+S_{nil}^{2x+}B_n^{j+\frac{1}{3}}\right)\frac{\beta_{n+1,il}^{j+\frac{1}{3}}-\beta_{nil}^{j+\frac{1}{3}}}{h_n^x}-\right.$$

$$-(S^{1x-}_{nil}R^{j+\frac{1}{3}}_{n-1}+S^{2x-}_{nil}B^{j+\frac{1}{3}}_{n-1})\frac{\beta^{j+\frac{1}{3}}_{nil}-\beta^{j+\frac{1}{3}}_{n-1,il}}{h^x_{n-1}}\Bigg]+\xi^j_{nil}, \tag{10}$$

$$\left(n=\overline{1,N-1};i=\overline{1,I-1};l=\overline{1,L-1}\right),$$

where

$$\omega^{j+1}_{nil}=\frac{\tau^{j+1}}{3V_{nil}},\qquad \xi^j_{nil}=\omega^{j+1}_{nil}\Bigg[\left(S^{1y+}_{nil}\widehat{R}^j_i+S^{2y+}_{nil}\widehat{B}^j_i\right)\frac{\beta^j_{n,i+1,l}-\beta^j_{nil}}{h^y_i}-$$

$$-\left(S^{1y-}_{nil}\widehat{R}^j_{i-1}+S^{2y-}_{nil}\widehat{B}^j_{i-1}\right)\frac{\beta^j_{nil}-\beta^j_{n,i-1,l}}{h^y_{i-1}}+$$

$$+\left(S^{1z+}_{nil}\widetilde{R}^j_l+S^{2z+}_{nil}\widetilde{B}^j_l\right)\frac{\beta^j_{ni,l+1}-\beta^j_{nil}}{h^z_l}-\left(S^{1z-}_{nil}\widetilde{R}^j_{l-1}+S^{2z-}_{nil}\widetilde{B}^j_{l-1}\right)\frac{\beta^j_{nil}-\beta^j_{ni,l-1}}{h^z_{l-1}}\Bigg].$$

The relation (10) is valid for internal cells of the domain Q. If any of the surfaces $S^{1x+}_{nil}, S^{1x-}_{nil}, ..., S^{2z-}_{nil}$ coincides with the outer boundary of the domain, then the corresponding term in the heat balance equation is approximated taking into account the boundary conditions. For this purpose, boundary conditions (2) on the outer boundary Γ are rewritten in the general form:

$$K(T)T_{\mathbf{n}}|_\Gamma=\left(r(T)T+q(t)\right)|_\Gamma.$$

Since

$$K(T)=\begin{cases}K_1(T), & (x,y,z)\in S^1_{nil},\\ K_2(T), & (x,y,z)\in S^2_{nil},\end{cases}=\begin{cases}\Omega_1(E), & (x,y,z)\in S^1_{nil},\\ \Omega_2(E), & (x,y,z)\in S^2_{nil},\end{cases}$$

the last expression splits into two equalities:

$$\Omega_1(E)\beta_{\mathbf{n}}(E)|_\Gamma=\left(r_1(\beta(E))\beta(E)+q_1(t)\right)|_\Gamma,\quad (x,y,z)\in S^1_{nil}, \tag{11}$$

$$\Omega_2(E)\beta_{\mathbf{n}}(E)|_\Gamma=\left(r_2(\beta(E))\beta(E)+q_2(t)\right)|_\Gamma,\quad (x,y,z)\in S^2_{nil}. \tag{12}$$

These relations are used to derive a spatial approximation of the heat fluxes on the outer boundary of the domain. For example, for $n=0$, system (10) must be supplemented by the equality:

$$E^{j+\frac{1}{3}}_{0il}-E^j_{0il}=\omega^{j+1}_{0il}\Bigg[(S^{1x+}_{0il}R^{j+\frac{1}{3}}_0+S^{2x+}_{0il}B^{j+\frac{1}{3}}_0)\frac{\beta^{j+\frac{1}{3}}_{1il}-\beta^{j+\frac{1}{3}}_{0il}}{h^x_0}\Bigg]+$$

$$+S^{1x-}_{0il}\left(r_1(\beta^{j+\frac{1}{3}}_{0il})\beta^{j+\frac{1}{3}}_{0il}+q^{j+\frac{1}{3}}_1\right)\Big|_{S^{1x-}_{0il}}+S^{2x-}_{0il}\left(r_2(\beta^{j+\frac{1}{3}}_{0il})\beta^{j+\frac{1}{3}}_{0il}+q^{j+\frac{1}{3}}_2\right)\Big|_{S^{2x-}_{0il}}+\xi^j_{0il}. \tag{13}$$

Let the function $\beta(E^j_{nil})$ be represented in the form:

$$\beta(E^j_{nil})=u^j_{nil}E^j_{nil}+v^j_{nil}, \tag{14}$$

where
$$u^j_{nil} = \begin{cases} \dfrac{1}{a_{nil}}, & E^j_{nil} < a_{nil}T_1, \\ \dfrac{1}{b^1_{nil}}, & a_{nil}T_1 \le E^j_{nil} < d^1_{nil}T_2 + d^2_{nil}, \\ \dfrac{1}{d^1_{nil}}, & E^j_{nil} \ge d^1_{nil}T_2 + d^2_{nil}, \end{cases}$$

$$v^j_{nil} = \begin{cases} 0, & E^j_{nil} < a_{nil}T_1, \\ \dfrac{b^2_{nil}}{b^1_{nil}}, & a_{nil}T_1 \le E^j_{nil} < d^1_{nil}T_2 + d^2_{nil}, \\ -\dfrac{d^2_{nil}}{d^1_{nil}}, & E^j_{nil} \ge d^1_{nil}T_2 + d^2_{nil}. \end{cases}$$

Then Eq. (10) can be rewritten as:

$$E^{j+\frac{1}{3}}_{nil} - E^j_{nil} = \omega^{j+1}_{nil} \frac{S^{1x+}_{nil} R^{j+\frac{1}{3}}_n + S^{2x+}_{nil} B^{j+\frac{1}{3}}_n}{h^x_n} \times$$

$$\times \left(u^{j+\frac{1}{3}}_{n+1,il} E^{j+\frac{1}{3}}_{n+1,il} + v^{j+\frac{1}{3}}_{n+1,il} - u^{j+\frac{1}{3}}_{nil} E^{j+\frac{1}{3}}_{nil} - v^{j+\frac{1}{3}}_{nil} \right) -$$

$$-\omega^{j+1}_{nil} \frac{S^{1x-}_{nil} R^{j+\frac{1}{3}}_{n-1} + S^{2x-}_{nil} B^{j+\frac{1}{3}}_{n-1}}{h^x_{n-1}} \left(u^{j+\frac{1}{3}}_{nil} E^{j+\frac{1}{3}}_{nil} + v^{j+\frac{1}{3}}_{nil} - u^{j+\frac{1}{3}}_{n-1,il} E^{j+\frac{1}{3}}_{n-1,il} - v^{j+\frac{1}{3}}_{n-1,il} \right) + \xi^j_{nil}.$$

The resulting system of nonlinear algebraic equations for $E^{j+\frac{1}{3}}_{nil}$ can be written as:

$$\hat{A}_n E^{j+\frac{1}{3}}_{n-1,il} - \hat{C}_n E^{j+\frac{1}{3}}_{nil} + \hat{B}_n E^{j+\frac{1}{3}}_{n+1,il} + \hat{D}_n = 0, \quad \left(n = \overline{1,N};\ i = \overline{0,I};\ l = \overline{0,L}\right). \tag{15}$$

Coefficients $\hat{A}_n, \hat{B}_n, \hat{C}_n$, and $\hat{D}_n$ are given in ([9]).

Taking into account (14), Eq. (13) for $n = 0$ is written as:

$$E^{j+\frac{1}{3}}_{0il} = n_0 E^{j+\frac{1}{3}}_{1il} + m_0, \quad i = \overline{0,I},\ l = \overline{0,L}. \tag{16}$$

The following relation for $n = N$ is derived by analogy with that for $n = 0$:

$$E^{j+\frac{1}{3}}_{Nil} = n_1 E^{j+\frac{1}{3}}_{N-1,il} + m_1, \quad i = \overline{0,I},\ l = \overline{0,L}. \tag{17}$$

Coefficients n_0, m_0, n_1, and m_1 are given in [9].

The resulting system of nonlinear algebraic equations (15)–(17) is divided into $(I+1)(L+1)$ subsystems. Each of them has the form of (15)–(17) with fixed indices $i \in \overline{0,I}$ and $l \in \overline{0,L}$ and is solved irrespective of the other subsystems by applying iteration and tridiagonal Gaussian elimination [8]. The coefficients $\hat{A}_n$, $\hat{B}_n$, $\hat{C}_n$, $\hat{D}_n$, n_0, m_0, n_1, and m_1 in the subsystems are determined by the calculated values of $E^{j+\frac{1}{3}}$ at the current iteration step. The value of $E^{j+\frac{1}{3}}$ at the next iteration step

is determined by tridiagonal Gaussian elimination. The iteration halts after the required accuracy was achieved.

The spatial approximations of the second and third subproblems are performed in a similar manner with the use of the solution obtained for the previous subproblems.

If the considered domain is more complex and consists of a set of different parallelepipeds (see Fig. 2), minor modifications of the algorithm described must be done. It should only be taken into account that the ranges of n, i, and l depend on the values of the pairs of numbers (i, l), (n, l), and (n, i) respectively.

4 Approximation of boundary conditions

The mold and the metal are cooled via their interaction with the surroundings. On the one hand, the object is slowly immersed in a liquid medium (aluminum) of a low temperature, due to which the metal solidifies. On the other hand, the body receives heat from the walls of the furnace, which slows down the process of solidification.

Therefore, the individual parts of the outer boundary of the body are in different thermal conditions. The basic types of thermal conditions at a point of the outer boundary of the body can be described as follows.

1) The point is in the liquid aluminum. In this case, the following processes have to be taken into account:
(i) the heat lost by the body due to its own radiation;
(ii) the heat gained from the surrounding liquid aluminum due to its radiation;
(iii) the heat transfer due to conduction between the liquid aluminum and the body.

2) The point is outside the liquid aluminum. In this case, the following processes have to be taken into account:
(i) the heat lost by the body due to its own radiation;
(ii) the heat gained from the emitting walls of the furnace;
(iii) the heat gained from the emitting surface of the liquid aluminum.

One of the mechanisms of heat transfer in this problem is thermal radiation. It can be computed as follows.

Consider two small areas (hereafter called elementary) in space (see Fig. 3). Let $\triangle s$ and $\mathbf{n}$ denote the size of the first area and its normal vector and $\triangle S$ and $\mathbf{N}$ denote the same characteristics for the second area. Assume that the first area emits thermal energy diffusely and its emissivity is ε. According to [10], the radiation energy flux $\triangle q$ from the first area of temperature T_{Sou} through the second area is calculated as

$$\triangle q = I\left(\mathbf{n}, \frac{\mathbf{r}}{|\mathbf{r}|}\right) \triangle s \triangle \omega,$$

where $I = \dfrac{1}{\pi}\varepsilon\sigma T_{Sou}^4$ is the intensity of the emission (σ is the Stefan-Boltzmann constant), $\triangle\omega$ is the solid angle at which the second area is seen from the center of the first area, and $\mathbf{r}$ is the position vector beginning from the center of the first

area and ending at the center of the second area (see Fig. 3). The solid angle $\triangle\omega$ is determined by the formula

$$\triangle\omega = \begin{cases} \dfrac{1}{|\mathbf{r}|^3}(\mathbf{N},\mathbf{r})\triangle S, & (\mathbf{N},\mathbf{r}) > 0, \\ 0, & (\mathbf{N},\mathbf{r}) \le 0. \end{cases}$$

Thus,

$$\triangle q = \frac{I(\mathbf{n},\mathbf{r})(\mathbf{N},\mathbf{r})}{|\mathbf{r}|^4}\triangle s\triangle S.$$

If radiation is emitted by an extended body s, the radiation energy flux q from it through the second elementary area is given by:

$$q = \triangle S \iint\limits_S \left(\frac{1}{\pi}\varepsilon\sigma T_{Sou}^4\right) \frac{(\mathbf{n}(y_1,y_2),\mathbf{r}(y_1,y_2))}{|\mathbf{r}(y_1,y_2)|^4}(\mathbf{N},\mathbf{r}(y_1,y_2))ds_y, \tag{18}$$

where $y = (y_1, y_2)$ are local coordinates introduced on the source surface s.

In the space under study, we introduce a Cartesian coordinate system with its origin at the center of $\triangle S$ and with the basis $\{\mathbf{e_1}, \mathbf{e_2}, \mathbf{e_3}\}$. Then the vector $\mathbf{N}$ normal to the second area can be expressed as $\mathbf{N} = N_1\mathbf{e_1} + N_2\mathbf{e_2} + N_3\mathbf{e_3}$. The flux q in (18) is represented by the sum of three fluxes:

$$q = [N_1q_1 + N_2q_2 + N_3q_3]\triangle S,$$

where

$$q_i = \iint\limits_S \left(\frac{1}{\pi}\varepsilon\sigma T_{Sou}^4\right) \frac{(\mathbf{n}(y_1,y_2),\mathbf{r}(y_1,y_2))}{|\mathbf{r}(y_1,y_2)|^4}(\mathbf{e_i},\mathbf{r}(y_1,y_2))ds_y.$$

The expressions for q_i $(i = 1, 2, 3)$ are derived assuming that the source surface is a rectangle. The basis vectors of the coordinate system are chosen so that they form a right-hand triple and $\mathbf{e_1}$ is orthogonal to the source plane and is directed toward it. Assume that the source has the size $l \times h$ and ξ is the distance from this source to the second elementary area.

a) The second elementary area is orthogonal to $\mathbf{e_1}$ (see Fig. 4). In this case, $\mathbf{N} = (1, 0, 0)$, $\mathbf{n} = (-1, 0, 0)$. Then

$$q_1 = M_0\left[\frac{h}{\sqrt{\xi^2+h^2}}\arctan\left(\frac{l}{\sqrt{\xi^2+h^2}}\right) + \frac{l}{\sqrt{\xi^2+l^2}}\arctan\left(\frac{h}{\sqrt{\xi^2+l^2}}\right)\right],$$

where $M_0 = \dfrac{1}{2\pi}\varepsilon\sigma T_{Sou}^4$.

b) The second elementary area is orthogonal to $\mathbf{e_2}$ (see Fig. 5). In this case, $\mathbf{N} = (0, 1, 0)$, $\mathbf{n} = (-1, 0, 0)$. Then

$$q_2 = M_0\left[\arctan\left(\frac{h}{\xi}\right) - \frac{\xi}{\sqrt{\xi^2+l^2}}\arctan\left(\frac{h}{\sqrt{\xi^2+l^2}}\right)\right].$$

c) The second elementary area is orthogonal to $\mathbf{e_3}$ (see Fig. 6). In this case, $\mathbf{N} = (0, 0, 1)$, $\mathbf{n} = (-1, 0, 0)$. Then

$$q_3 = M_0 \left[\arctan\left(\frac{l}{\xi}\right) - \frac{\xi}{\sqrt{\xi^2 + h^2}} \arctan\left(\frac{l}{\sqrt{\xi^2 + h^2}}\right) \right].$$

Now, let's take a closer look at the description of the boundary conditions (11) and (12), i.e. at a more detailed description of the functions $r_1(\beta(E))$, $q_1(t)$, $r_2(\beta(E))$, and $q_2(t)$. For the sake of simplicity, the description of these functions is given for a rectangular parallelepiped.

Consider the face of the parallelepiped which is parallel to the plane YOZ and is located closer to the right wall of the furnace (Fig. 1). As noted above, some areas of this face can be in different thermal conditions.

For the considered face of the object all the cells are filled with the material of the form. The considered face consists of this cell's surfaces that are designated as S^{2x+}_{Nil}, $(i = \overline{0, I}, \quad l = \overline{0, L})$. For the time $t = t^j$, when the cell is located outside of the liquid aluminum we have:

$$\Omega_2(E^j_{Nil})\beta_{\mathbf{n}}(E^j_{Nil})\Big|_{S^{2x+}_{Nil}} = -\sigma \cdot \left(\beta^j_{Nil}\right)^4 + \varphi_s + \varphi_a, \tag{19}$$

where φ_s is the radiation energy flux density of the whole right wall through the surface S^{2x+}_{Nil} (let us note that in this case the radiation from the left wall of the furnace does not fall on the considered face of object), and φ_a is the radiation energy flux density from the surface of liquid aluminum through this surface. The values φ_s and φ_a are calculated by the formulas:

$$\varphi_s = q_s(X_s, Y_{Sou} - y_i + L_{Sou}, Z_{Sou} - z_l + H_{Sou}) - q_s(X_s, Y_{Sou} - y_i, Z_{Sou} - z_l + H_{Sou}) +$$
$$+ q_s(X_s, Y_{Sou} - y_i, Z_{Sou} - z_l) - q_s(X_s, Y_{Sou} - y_i + L_{Sou}, Z_{Sou} - z_l), \tag{20}$$

$$\varphi_a = q_a(Z_a, Y_{al} - y_i + L_{al}, X_{al} - X_b + H_{al}) - q_a(Z_a, Y_{al} - y_i, X_{al} - X_b + H_{al}). \tag{21}$$

Here:
X_s is the distance from the surface S^{2x+}_{Nil} of the considered cell to the nearest wall of the furnace,
(X_B, y_i, z_l) are the coordinates of center of the surface of the considered cell,
Y_{Sou} is the ordinate of the lower vertex of the right wall of the furnace, nearest to the point of origin O of the selected coordinate system,
Z_{Sou} is the z-coordinate of the lower bound of the wall of the furnace at the moment $t = t^j$,
X_{al}, Y_{al} are the abscess and the ordinate of the vertex of the surface of aluminum, nearest to the point of origin O of the selected coordinate system,
$Z_a = z_l - U_{al}$ is the distance from the surface S^{2x+}_{Nil} of the considered cell to the surface of the liquid aluminum,

$$U_{al} = \begin{cases} Z_{al}, & \text{object did not reach the surface of aluminum,} \\ Z_{al} + \dfrac{X_b \cdot Y_b \cdot Z_{al}}{L_{al} \cdot H_{al} - X_b \cdot Y_b}, & \text{object reached the surface of aluminum,} \end{cases}$$

$Z_{al} = Z_{Sou} - H_{air}$,
X_b is the length of the parallelepiped along the Ox axis,
Y_b is the length of the parallelepiped along the Oy axis,
Z_b is the height of the parallelepiped along the Oz axis,
L_{Sou} is the length of the plate of the furnace along the Oy axis,
H_{Sou} is the height of the plate of the furnace along the Oz axis,
H_{air} is the distance from the furnace to the liquid aluminum,
L_{al} is the length of the aluminum surface along the Oy axis,
H_{al} is the length of the aluminum surface along the Ox axis.
Functions q_s and q_a are determined using the following formulas:

$$q_s(\xi, l, h) = M_s \cdot \left[\frac{h}{\sqrt{\xi^2 + h^2}} \arctan\left(\frac{l}{\sqrt{\xi^2 + h^2}} \right) + \frac{l}{\sqrt{\xi^2 + l^2}} \arctan\left(\frac{h}{\sqrt{\xi^2 + l^2}} \right) \right], \tag{22}$$

$$q_a(\xi, l, h) = M_a \cdot \left[\arctan\left(\frac{l}{\xi} \right) - \frac{\xi}{\sqrt{\xi^2 + h^2}} \arctan\left(\frac{l}{\sqrt{\xi^2 + h^2}} \right) \right], \tag{23}$$

where $M_s = \dfrac{1}{2\pi} \varepsilon_s \sigma T_{Sou}^4$, $M_a = \dfrac{1}{2\pi} \varepsilon_a \sigma T_{al}^4$, T_{Sou} is the temperature of the plate of the furnace, T_{al} is the temperature of the liquid aluminum, ε_s is emissivity of the wall of the furnace, ε_a is emissivity of the liquid aluminum.

When the cell is places outside the liquid aluminum then according to (12) and (19) we have:

$$r_2\left(\beta(E_{Nil}^j)\right)\Big|_{S_{Nil}^{2x+}} = -\sigma \cdot (\beta_{Nil}^j)^3, \qquad q_2(t)|_{S_{Nil}^{2x+}} = \varphi_s + \varphi_a.$$

When the cell is places inside the liquid aluminum we have:

$$\Omega_2(E_{Nil}^j)\beta_{\mathbf{n}}(E_{Nil}^j)\Big|_{S_{Nil}^{2x+}} = -\lambda \cdot (\beta_{Nil}^j - T_{al}) - \sigma \cdot (\beta_{Nil}^j)^4 + \sigma \cdot (T_{al})^4,$$

and accordingly

$$r_2\left(\beta(E_{Nil}^j)\right)\Big|_{S_{Nil}^{2x+}} = -\left(\sigma \cdot (\beta_{Nil}^j)^3 + \lambda\right), \quad q_2(t)|_{S_{Nil}^{2x+}} = \lambda \cdot T_{al} + \sigma \cdot (T_{al})^4.$$

Here λ is the coefficient of heat exchange between the object and the liquid aluminum. Boundary conditions for the remaining five faces of the parallelepiped are approximated analogously. The upper face of the parallelepiped is differed from the rest because the outer boundary consists of both the cells containing the material of the form and the cells containing the material of the metal, i.e. in this case both conditions (11) and (12) operate.

5 Numerical results of solving the direct problem

First, the direct problem was studied for an object of the simplest shape – a rectangular parallelepiped. This object was used to test and tune the algorithms proposed for solving the problem.

The direct problem was also solved for an actual object. Its longitudinal projections are displayed in Fig. 2. This object had two planes of symmetry and was located symmetrically in the furnace. It consisted of five parallelepipeds. The exterior view of its quarter is shown in Fig. 7. The object was immersed in the molten aluminum up to the fourth parallelepiped. The speed $\widetilde{u}(t)$ of the displacement of foundry mold was relied equal to zero, when it reached the maximum permissible depth.

The numerical results presented below were obtained for this object and for the following parameter values (given in SI units):

$\rho_S = 8200.0,$	$k_S = 23.3,$	$c_S = 670.0,$	$\rho_L = 7200.0,$
$k_L = 15.2,$	$c_L = 790.0,$	$\rho_\Phi = 2700.0,$	$k_{\Phi_1} = 4.7,$
$k_{\Phi_2} = 3.2,$	$c_\Phi = 780.0,$	$T_1 = 1493.15,$	$T_2 = 1633.15,$
$T_3 = 1100.15,$	$\delta = 20.0,$	$\gamma = 234000.0,$	$T_{met} = 1973.15,$
$T_{form} = 1853.15,$	$L_{al} = 0.500,$	$H_{al} = 0.300,$	$H_{air} = 0.070,$
$T_{Sou} = 1823.15,$	$T_{al} = 1003.15,$	$L_{Sou} = 0.450,$	$H_{Sou} = 0.535,$
$\lambda = 1.0,$	$\varepsilon_s = 0.8,$	$\varepsilon_a = 0.8,$	$T_{pl} = 0.5(T_1 + T_2),$

$X_b = 0.07$ (the length of a quarter of the casting along the Ox axis),
$Y_b = 0.1$ (the length of a quarter of the casting along the Oy axis),
$Z_b = 0.435$ (the length of the casting along the Oz axis).

The number t^J which determines the length of the interval of time $[0, t^J]$ was selected so that the time during which the complete solidification of the metal in the foundry mold occurs would not exceed the value t^J for all considered regimes of the process of crystallization.

In the computation of the direct problem, primary attention was given to the evolution of the solidification front. The dependance of this evolution as a function of the velocity of the object is illustrated in Figures 8–15, which show lines of constant temperature at different times in two cross sections ((a) and (b)) through the object's vertical axis of symmetry parallel to the object faces. Since the object is symmetric about the vertical axis, the figures present only halves of the cross sections. The light vertical and horizontal lines inside the object separate the metal and the mold. The light curves show lines of constant temperature, and the heavy curve depicts the contour line of $T = T_{pl}$. It separates the liquid and solid phases in the metal. The figures with different numbers correspond to different times. Figures 8–11 (first experiment) illustrate the process of metal solidification in a mold moving relative to the furnace at the constant speed $\widetilde{u}(t) = 2$ mm/min. In the second experiment (Figures 12–15), the speed was piecewise constant. More specifically, it remained constant in three time intervals. Over the first time interval, the first (narrowest) parallelepiped was immersed in the coolant at the speed 20 mm/min. Over the second and third time intervals, the second and third parallelepipeds were immersed in the coolant at the speeds 10 and 5 mm/min respectively. Poor results were obtained when the object moved at a constant low speed. The solidification of the metal proceeded from two sides (lower and upper). This led to the formation of bubbles of liquid metal that collapse inside the casting. It should be noted that

the solidification front was nearly always far from a horizontal plane. In the second experiment, the solidification front always intersected the metal transversally only once and was noticeably more similar to a horizontal plane. No bubbles of liquid metal were observed inside the casting during the entire process.

Acknowledgments. This work was supported by the Russian Foundation for Basic Research (project no. 08-01-90100-Mol_a) and the program "Leading Scientific Schools" (project no. NSh-5073.2008.1).

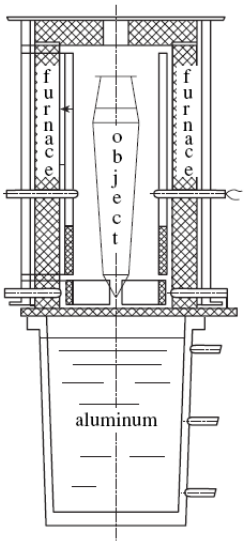

Fig. 1

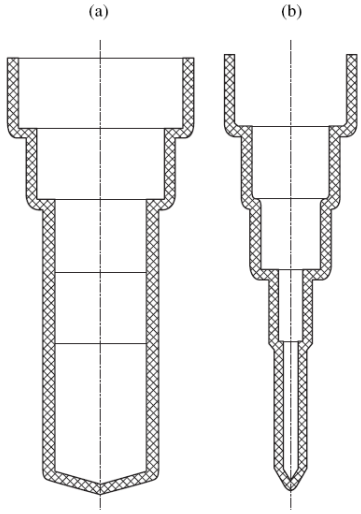

Fig. 2

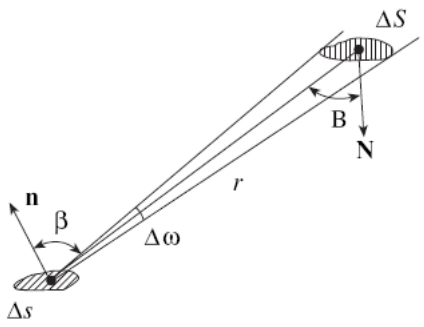

Fig. 3

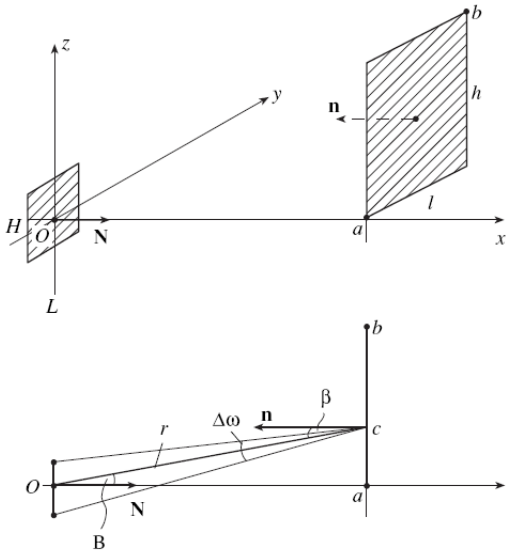

Fig. 4

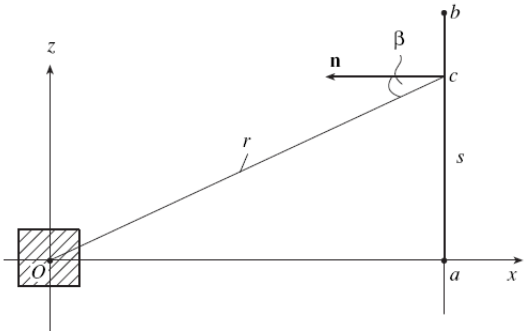

Fig. 5

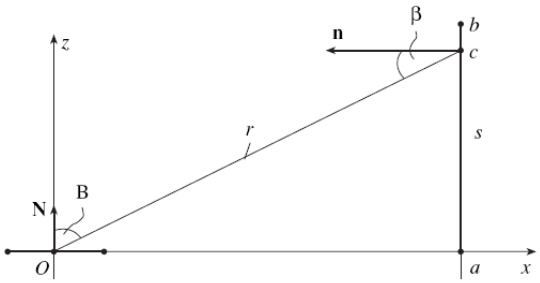

Fig. 6

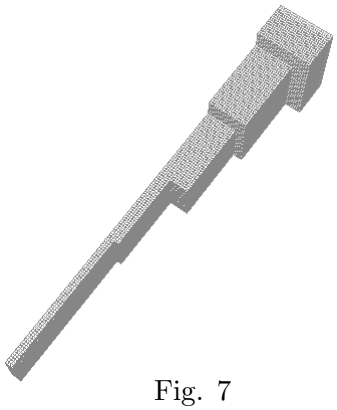

Fig. 7

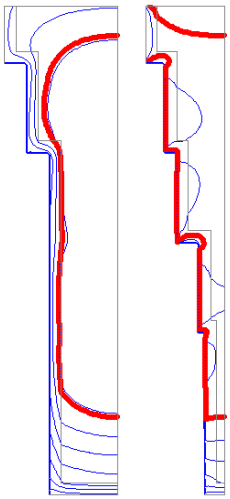

Fig. 8 a,b

Fig. 9 a,b

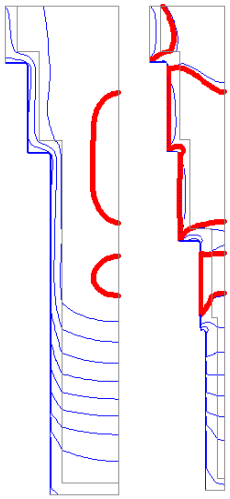

Fig. 10 a,b

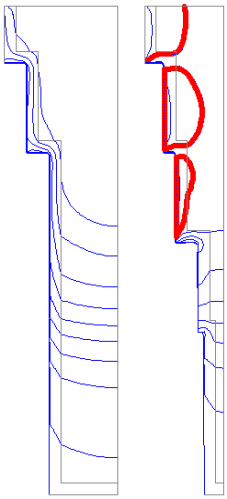

Fig. 11 a,b

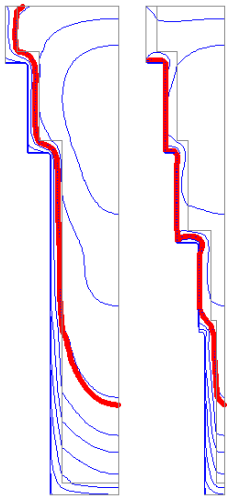

Fig. 12 a,b

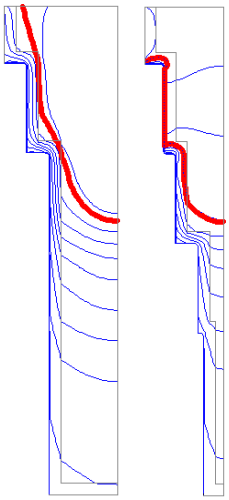

Fig. 13 a,b

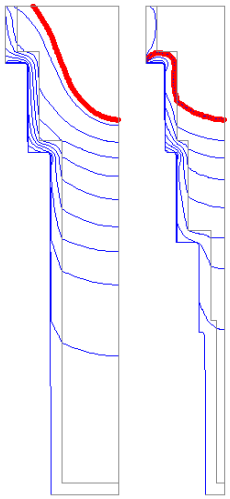

Fig. 14 a,b

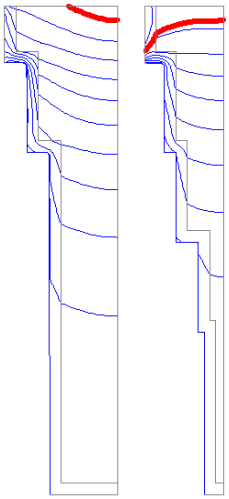

Fig. 15 a,b

References

[1] Rose M.E. *A method for calculating solutions of parabolic equations with a free boundary.* Math. Comput., 1960, **14**, 249–256.

[2] White R.E. *An Enthalpy Formulation of the Stephan Problem.* SIAM J. Numer. Anal., 1982, **19**, No. 6, 1129–1157.

[3] White R.E. *A numerical solution of the enthalpy formulation of the Stephan problem.* SIAM J. Numer. Anal., 1982, **19**, No. 6, 1158–1172.

[4] Albu A.F., Gorbunov V.I., Zubov V.I. *Optimal Control of the Process of Melting.* Zh. Vychisl. Mat. Mat. Fiz., 2000, **40**, No. 4, 517–531 (Comp. Math. Math. Phys., 2000, **40**, 491–504).

[5] Albu A.F., Zubov V.I. *A Modified Scheme for Analyzing the Process of Melting.* Zh. Vychisl. Mat. Mat. Fiz., 2001, **41**, No. 9, 1434–1443 (Comp. Math. Math. Phys., 2001, **41**, 1363–137).

[6] Albu A.F., Zubov V.I. *Optimal Control of the Process of Solidification.* Zh. Vychisl. Mat. Mat. Fiz., 2004, **44**, No. 1, 38–50 (Comp. Math. Math. Phys., 2004, **44**, 34–44).

[7] Albu A.F. and Zubov V.I. *Modeling and optimization of melting and solidification process.* Buletinul Academiei de Ştiinţe a Republicii Moldova. Matematica, 2004, No. 3(46), 91–109.

[8] Samarskii A.A. *The Theory of Difference Schemes.* Marcel Dekker, New York, 2001.

[9] Albu A.F., Zubov V.I. *Mathematical modeling and study of the process of solidification in metal casting.* Zh. Vychisl. Mat. Mat. Fiz., 2007, **47**, No. 5, 882–902 (Comp. Math. Math. Phys., 2007, **47**, 843–862).

[10] Sparrow E.M., Cess R.D. *Radiation Heat Transfer.* Brooks-Cole, Belmont, Calif., 1972.

V. I. Zubov
Computing Centre of Russian Academy of Sciences
40, Vavilova Str., 119333, Moscow
Russia

E-mail: *zubov@ccas.ru*

Received October 9, 2008